## Nature of Bosonic Excitations revealed by high-energy charge carriers

Jan Kogoj, <sup>1</sup> Marcin Mierzejewski, <sup>2</sup> and Janez Bonča<sup>1, 3</sup>

<sup>1</sup> J. Stefan Institute, 1000 Ljubljana, Slovenia

<sup>2</sup> Institute of Physics, University of Silesia, 40-007 Katowice, Poland

<sup>3</sup> Faculty of Mathematics and Physics, University of Ljubljana, 1000 Ljubljana, Slovenia

We address a long standing problem concerning the origin of bosonic excitations that strongly interact with charge carriers. We show that the time-resolved pump-probe experiments are capable to distinguish between regular bosonic degrees of freedom, e.g. phonons, and the hard-core bosons, e.g., magnons. The ability of phonon degrees of freedom to absorb essentially unlimited amount of energy renders relaxation dynamics nearly independent on the absorbed energy or the fluence. In contrast, the hard core effects pose limits on the density of energy stored in the bosonic subsystems resulting in a substantial dependence of the relaxation time on the fluence and/or excitation energy. Very similar effects can be observed also in a different setup when the system is driven by multiple pulses of equal energy.

Solids are complex objects with different degrees of freedom, hence the charge carriers are simultaneously coupled to various types of bosonic excitations like phonons, magnons, plasmons or others. The longstanding problem in the studies on strongly correlated systems is to single out the strongest, and thus probably the most relevant interaction. However for many important materials, including the unconventional superconductors, we are still seeking the answer to a more modest question, whether the strongest coupling of charge carriers is to phonons or to some kind of magnetic excitations. The essential qualitative difference between these excitations is that the latter ones are hard-core (HC) quasiparticles, i.e. their spatial density is limited typically by one boson per lattice site. It is rather clear that the HC effects become important first in the vicinity of this bound, i.e. when the energy density is of the order of the frequency of the bosonic excitations. However, it might be impossible to heat up the entire system to such high energies since, e.g., the corresponding temperature may be too close to the melting point. A very promising solution is to excite only targeted degrees of freedom. Directly after such excitation, the total system is far from equilibrium since various degrees of freedom may have very different temperatures (energies to be more precise).

This solution is utilised in the recent time resolved photoemission and optical spectroscopies, where one studies ultrafast relaxation of a few highly excited charge carriers [1–9]. These carriers lower high initial kinetic energy (of the order of 1-2eV) in a narrow time-window, by emitting many of most strongly coupled bosons. In the vicinity of the excited charge carriers, the concentration of emitted bosons may be high enough so that the HC effects become visible.

In the majority of the recent theoretical papers, the ultrafast relaxation of highly excited carriers has been discussed separately for the couplings to phonons [10–24] and to the magnetic excitations [25–28]. On the one hand, the electron-phonon coupling is usually described within the Holstein model by two independent parameters: the dimensionless coupling strength,  $\lambda$  and the phonon frequency,  $\omega$ . The electron-phonon interaction

is efficient in any dimension, hence it has been mostly studied in the simplest case of the one-dimensional (1D) systems. On the other hand, the coupling to the magnetic excitations is studied mainly within the Hubbard or the t-J models. Each of the latter models contains a single free parameter (U/t or J/t) which encodes the coupling strength as well as the frequency of the excitations. Since the spin and the charge degrees of freedom are separated in the 1D systems, relaxation due to magnetic excitations should be studied at least in two dimensions. Due to the essential differences between the studied models, it is difficult to specify the distinctive qualitative features of both mechanisms. In the present work we fill this important gap. We compare the relaxation of charge carriers in two models, chosen such that all the emerging differences are solely due to HC effects of the bosonic excitations. We show that if the relaxation is due to the coupling to HC bosons, then the relaxation time shows pronounced dependence on the excitation energy and/or the density of excited carriers. The opposite holds true for coupling do standard bosonic degrees of freedom.

Model. We consider two models on a one-dimensional ring with L sites, each containing a single electron. The first one is the Holstein model (HM) while the second is a HC boson model (HCM) where phonon degrees of freedom are replaced by hard core bosons. Hamiltonians of both models have a very similar structure:

$$H_{\text{svs}} = H_{\text{kin}} + H_{\text{bos}} + H_{\text{int}},\tag{1}$$

where individual part of  $H_{\text{sys}}$  are as follows:

$$H_{\text{kin}} = -t_0 \sum_{j} \left( e^{i\phi(t)} c_j^{\dagger} c_{j+1} + \text{h.c.} \right)$$

$$H_{\text{bos}} = \omega \sum_{j} b_j^{\dagger} b_j, \qquad (2)$$

$$H_{\text{int}} = -g \sum_{j} c_j^{\dagger} c_j (b_j^{\dagger} + b_j), \qquad (3)$$

where  $t_0$  is the hopping amplitude, and  $c_j$  is a fermion

annihilation operator on site j. Operators  $b_j$  represent either phonon or HC boson field annihilation operator. There is at most one HC boson per site, hence  $b_i^{\dagger}b_i^{\dagger}=0$ . This restriction shows up in specific commutation relations  $[b_i,b_j^{\dagger}]=\delta_{ij}(1-2b_i^{\dagger}b_i)$  for the latter operators. For clarity of comparison we introduce identical dispersionless frequency  $\omega$  and coupling g for phonons and HC bosons alike. The  $\phi(t)$  represents the phase gained by the electron as it hops between successive sites. It is used to pump energy into the system as described in the last part of this work. We measure time in units  $\hbar/t_0$  and set  $\hbar=1$ .

We solve both models using the Lanczos-based diagonalization defined within a limited functional space (LFS) to obtain the ground state as well as for the time evolution. The generation of the LFS efficiently selects states with different phonon configurations in the vicinity of the electron thus enabling numerically exact solution of the polaron problem [29, 30], and it is well-suited also to describe polaron systems far from the equilibrium [10, 21, 31, 32]. A detailed description of this numerical approach can be found in Ref. [31].

In the first part of this work we start the time evolution from the free electron wavefunction at a given wave number k,  $|\psi_0(t=0)\rangle = c_k^\dagger |0\rangle$  where  $|0\rangle$  represents vacuum state for electrons and bosons. We choose the initial kinetic energy of the electron  $E_{\rm kin}(t=0) = -2t_0\cos(k)$  to be much larger than the ground-state  $E_{\rm kin}^{\rm GS}$  of the polaron. We then perform the time evolution under  $H_{\rm sys}$ , Eq. 1, to obtain the wavefunction  $|\psi(t)\rangle$  of the system. This approach simulates polaron formation starting from a free electron with variable (possibly very high) initial kinetic energy.

In Fig. 1(a) we present comparison of  $E_{\rm kin}(t) = \langle H_{\rm kin}(t) \rangle$  of HM and HCM for different values of initial k. In all cases we observe a decrease of  $E_{\rm kin}(t)$  towards a quasi steady state values  $\bar{E}_{\rm kin}$  that remain consistently above their respective ground-state values  $E_{\rm kin}^{\rm GS}$ . We should stress that the total energy of the system  $E_{\rm sys}$  remains constant during the time evolution and it equals the initial value of the kinetic energy, *i.e.*  $E_{\rm sys} = E_{\rm kin}(t=0)$ . The decrease of  $E_{\rm kin}(t)$  is thus intimately connected to the increase of the phonon or HC boson energy. The main difference between the models under consideration is that phonon degrees of freedom can absorb in principle an infinite amount of energy while HC bosons can absorb at most  $\omega$  of energy per site.

To facilitate further comparison of relaxation dynamics between two different models, we have shifted all initial values of  $E_{\rm kin}$  to  $E_{\rm kin}(t=0)=0$ , see Fig. 1(b). For small k, i.e.  $k=\pi/2$  and  $5\pi/8$ , relaxation dynamics of HM and HCM are nearly indistinguishable. For larger values of  $k\geq 3\pi/4$ , however, relaxation of the HM seems to be substantially faster than that of the HCM. Nevertheless, the quasi-steady state values  $\bar{E}_{\rm kin}$  are nearly indistinguishable between the two models. Even though the relaxation process is not strictly exponential, we nevertheless found very reasonable exponential fits to the data,

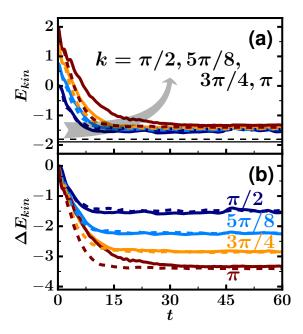


FIG. 1.  $E_{\rm kin}(t)$  vs. time t for different values of k in (a) and  $\Delta E_{\rm kin}(t) = E_{\rm kin}(t) - E_{\rm kin}(t=0)$  in (b). Dashed (full) lines are represent results for HM (HCM). Other parameters of the Hamiltonian in Eq. 2 are  $\omega=0.5,\ g=\sqrt{0.5}$  and the size of the system with periodic boundary conditions is L=16. Unless otherwise specified, identical parameters were used in all subsequent figures. The phase is set to  $\phi(t)=0$  in all figures but Fig 5. Thin horizontal lines present ground-state kinetic energies  $E_{\rm kin}^{\rm GS}$ .

presented in Fig. 1(b).

In Fig. 2 we present the central result of this work, that is, the comparison of relaxation times  $\tau_{\rm HM}$  and  $\tau_{\rm HCM}$ of the HM and HCM, respectively as a function of the quench energy that is defined as a difference between the initial kinetic energy of the electron and the average kinetic energy in the quasi steady state:  $\Delta = E_{\rm kin}(t)$  $0) - \bar{E}_{\rm kin}$ . We found a relatively weak dependence of relaxation times  $\tau_{\rm HM}$  on  $\Delta$  in particular, there is no abrupt raise of  $\tau_{\rm HM}$  at large values of  $\Delta$ . In contrast, much more pronounced dependence on  $\Delta$  is found in the case of  $\tau_{\rm HCM}$ , see Fig. 2. We observe a sharp up-turn of  $\tau_{\rm HCM}$  for larger values of  $\Delta$  signalling a significant slowing down of the relaxation process in the HCM. In contrast, at small  $\Delta \sim 1.5$ ,  $\tau_{\rm HCM}$  approaches  $\tau_{\rm HM}$ . We should also stress, that relaxation times for  $\Delta \lesssim 2$  become less reliable since relaxation processes evolve over a smaller number of eigenstates. The dependence of  $\Delta$  on the wave vector k is presented in the insert of Fig. 2.

To gain a deeper understanding of the different relaxation processes in models under the investigation, we computed the average number of bosonic excitations per site, given by  $n_{\text{bos}} = \langle \psi(t) | \sum_i b_i^{\dagger} b_i | \psi(t) \rangle / L$ , shown in Fig. 3. We first note that there is no upper bound on  $n_{\text{bos}}$  in the HM case. In contrast, there is a formal upper bound  $n_{\text{bos}} \leq 1$  in the HCM while twice smaller

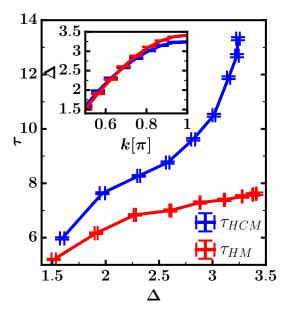


FIG. 2. Relaxation time  $\tau_{\rm HM}$  ( $\tau_{\rm HCM}$ ) for HM (HCM) vs. quench energy  $\Delta$ .  $\tau$  were extracted from data presented in Fig. 1(b) using the following analytical form  $\Delta E_{\rm kin}(t) = A \exp{[-t/\tau]} + B$ . In the inset we show the dependence of  $\Delta$  on the wave number of the initial free electron wavefunction k.

concentration  $n_{\text{bos}} = 0.5$  is reached only in the limit of infinite temperature. In both models we observe an increase of  $n_{\rm bos}$  at longer times as the k and with it  $\Delta$ increase. While  $n_{\text{bos}}$  in the HM keeps increasing with increasing k, we observe signs of saturation in the HCM case as  $n_{\rm bos}$  moves closer to its infinite–temperature value  $n_{\rm bos} = 0.5$  at maximal quench energy reached at  $k = \pi$ . In the HM we observe pronounced oscillations in the long-time regime with the time-period  $t_p \sim 2\pi/\omega$  that are not reflected in oscillations of  $E_{\rm kin}(t)$  since they are compensated by oscillations in the interaction energy  $E_{\rm int} = \langle H_{\rm int} \rangle$ , not shown. We observe also that  $n_{\rm bos}$ in the HM systematically substantially exceeds  $n_{\rm bos}$  in the HCM. Taking also into account that total energies of both models together with nearly equal  $E_{\rm kin}$ , see Fig. 1, a large difference in  $n_{\rm bos}$  represents a seeming contradiction. Nevertheless, the excess in bosonic energy is compensated by a lower interaction energy  $E_{\text{int}}$  (not shown) in the HM.

We next present in Fig. 4(a) surface plots of the correlation function

$$\gamma(j,t) = \langle \psi(t) | \sum_{i} c_i^{\dagger} c_i b_{i+j}^{\dagger} b_{i+j} | \psi(t) \rangle.$$
 (4)

 $\gamma(j,t)$  enables us to follow the spread of bosonic degrees of freedom during the time evolution. At short times,  $t \lesssim 5$  and small intensities,  $\gamma(j,t) \lesssim 0.1$ , we observe a similar spread of the front of bosonic excitations away from the electron position at j=0. This spread is given by the Lieb-Robinson's velocity (i.e., the maximal speed at which information propagates) that in both models

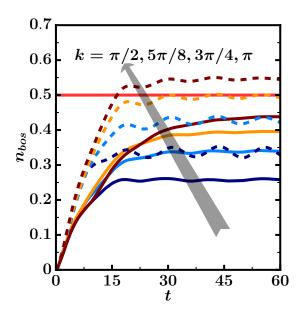


FIG. 3. Average number of bosonic excitations per-site  $n_{\rm bos}$  vs. t for different values of k corresponding to different  $\Delta$  as depicted in the inset of Fig. 2. Dashed (full) lines represent results for the HM (HCM). The horizontal line indicates the infinite–temperature value of  $n_{\rm bos}$  in the HCM.

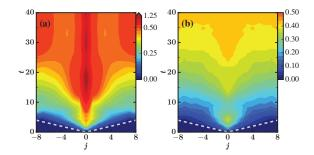


FIG. 4. Density plot of the spread of bosonic excitations  $\gamma(j,t)$  for the HM in a) and HCM in b) for  $k=\pi$ . Dashed white lines represent the Lieb Robinson bound as described in the text. To facilitate a straightforward comparison between models, identical colour coding was used in both figures.

equals the maximal velocity of a free electron  $v_{\rm LR}=2t_0$ . Since bosons of both types are dispersionless, the observed velocity is due to the electron that moves away from the bosonic excitation. At later times and larger intensities we observe a qualitative difference in  $\gamma(j,t)$  between both models. In the HM there is an excess of extra phonon excitations at and in the close proximity of the electron's position. In contrast, the HCM case bosonic degrees of freedom spread much more uniformly throughout the entire system. This represents the main mechanism that causes substantial slowing down of relaxation in HCM at larger values of  $\Delta$ . As  $\Delta$  increases far beyond the typical bosonic frequency,  $\Delta \gtrsim \omega_0$ , in a semiclassical picture, the charge has to to travel ever larger distance to dispose off the excess energy.

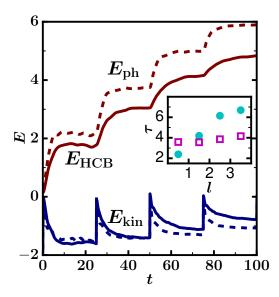


FIG. 5. Kinetic energy  $E_{\rm kin}$ , phonon energy  $E_{\rm ph}$  and hard core boson energy  $E_{\rm HCB}$  vs time. Dashed (full) lines represent results for the HM (HBM).  $\omega=g=0.75$ , and L=16 was used in this particular case. Note that the upper limit of  $E_{\rm HCB}$ , reached at infinite temperature, is  $E_{\rm HCB}^{\rm max}=L\omega/2=6$ . Multiple spikes in  $E_{\rm kin}$  are due to step-like jumps in the phase  $\phi(t)=\pi/2\sum_{l=0}^3\theta(t-l\Delta t)$  where  $\Delta t=25$  and  $\theta(x)$  is the Heaviside step function. In the insert we present relaxation time  $\tau$  with squares (full circles) for the HM (HBM), extracted from the relaxation of  $E_{\rm kin}(t)$  in distinct time intervals between successive step-like changes of  $\phi(t)$ .

We have demonstrated that the HC effects slow down the relaxation of highly exited charge carriers. Therefore, the future experiments showing the relaxation time vs. the excitation energy may shed light on the type of bosons, which are most strongly coupled to the carriers. However, in the majority of the experimental setups it is easy to tune the density of photoexcited carriers (e.g., by changing the fluence) but not necessarily their energy. Direct numerical simulations of the former problem cannot be carried out within the present model with a single charge carrier. However, we expect that a qualitatively similar picture may be obtained from the studies of a slightly different experimental setup when a charge carrier is driven by multiple pulses. The discussed scenario should hold independently of whether the bosons are excited by a single or various charge carriers. At the end, what matters for the hard-core effects is the density of the bosons and not their source.

In Fig. 5 we show how the relaxation changes upon applying subsequent pulses to HM and HCM. We have simulated this case by starting the time evolution from the polaron ground state wavefunction at  $t=0^-$ , followed by successive step-like jumps in the phase  $\phi(t)$  as described in the caption of Fig. 5. Each jump in  $\phi(t)$  causes an abrupt jump of  $E_{\rm kin}$  followed by a relaxation process in which a decrease in  $E_{\rm kin}$  is followed by the increase of the corresponding boson energy. In the HCM,

the relaxation after succeeding pulses becomes visibly slower as the density of excited hard–core bosons becomes comparable with its value at infinite temperature, i.e.  $E_{\rm HCM}^{\rm max}/L=\omega/2$ , see also the caption in Fig. 5 In contrast, relaxation in the HM does not show any substantial dependence on the number of preceding pulses. This is clearly seen in the insert of Fig. 5 where we present relaxation times for both models as extracted from the exponential fits to  $E_{\rm kin}$  in distinct time intervals.

In summary, we propose a simple mechanism to distinguish between two different classes of bosonic excitations that are responsible for the primary (fastest) relaxation mechanism of a photo excited charge carrier in time-resolved pump-probe experiments. The proposed mechanism is based on the recognition that phonon degrees of freedom can absorb essentially unlimited amount of energy while in contrast, the hard core effects, typical for e.g. magnon excitations, pose strict limits on the density of absorbed energy. For this reason the relaxation dynamics of the charge carrier coupled to phonon degrees of freedom very weakly depends on the excitation energy, while the opposite is true when the charge carrier is coupled to HC boson excitations. In the latter case the relaxation becomes less effective when the absorbed energy approaches the typical HC boson frequency, i.e.  $\Delta \sim \omega$ . The density of excited bosons can be tuned either by changing the fluence of a single pumppulse, or by driving the system by multiple pulses. In the latter case the time span between the first and the last pulses should be significantly smaller than the secondary relaxation time when other, weakly coupled degrees of freedom start to influence the relaxation process.

To gain clear distinction between the two different cases, we performed simulations on nearly identical models containing either Einstein phonons or dispersionless HC bosons. However, in more realistic systems dispersionless HC bosons should be replaced by, e.g., dispersive magnetic excitations with a given magnon velocity  $v_{\rm mag}$ . Still, even in this case the slowing down of relaxation due to HC effects is expected in two spacial dimensions when  $\Delta \sim \omega (v_{\rm mag} \tau)^2$ . Up to our best knowledge, the predictions of this work have not been yet tested experimentally. However, the very recent experiments on cuprates show significant fluence-dependence of the relaxation times obtained for the electron-states which are far above the Fermi energy (see Fig. 5 in Ref. [8]). This result suggests that in cuprates the charges are most strongly-coupled to HC bosonic excitation, which are most probably of the magnetic origin.

## ACKNOWLEDGMENTS

We acknowledge stimulating discussions with U. Bowensiepen, C. Giannetti. J.B. acknowledges discussions with A. Polkovnikov and M. Rigol as well as the support by the P1-0044 of ARRS, Slovenia. M.M. acknowledges support from the DEC-

2013/11/B/ST3/00824 project of the Polish National Science Center. J.K. acknowledges financial assistance by the Alexander von Humboldt Foundation. This work

was performed, in part, at the Center for Integrated Nanotechnologies, a U.S. Department of Energy, Office of Basic Energy Sciences user facility.

- [1] H. Okamoto, T. Miyagoe, K. Kobayashi, H. Uemura, H. Nishioka, H. Matsuzaki, A. Sawa, and Y. Tokura, Ultrafast charge dynamics in photoexcited Nd<sub>2</sub>CuO<sub>4</sub> and La<sub>2</sub>CuO<sub>4</sub> cuprate compounds investigated by femtosecond absorption spectroscopy, Phys. Rev. B 82, 060513 (2010).
- [2] C. Gadermaier, A. S. Alexandrov, V. V. Kabanov, P. Kusar, T. Mertelj, X. Yao, C. Manzoni, D. Brida, G. Cerullo, and D. Mihailovic, Electron-phonon coupling in high-temperature cuprate superconductors determined from electron relaxation rates, Phys. Rev. Lett. 105, 257001 (2010).
- [3] R. Cortés, L. Rettig, Y. Yoshida, H. Eisaki, M. Wolf, and U. Bovensiepen, Momentum-resolved ultrafast electron dynamics in superconducting bi<sub>2</sub>sr<sub>2</sub>cacu<sub>2</sub>o<sub>8+δ</sub>, Phys. Rev. Lett. 107, 097002 (2011).
- [4] S. Dal Conte, C. Giannetti, G. Coslovich, F. Cilento, D. Bossini, T. Abebaw, F. Banfi, G. Ferrini, H. Eisaki, M. Greven, A. Damascelli, D. van der Marel, and F. Parmigiani, Disentangling the electronic and phononic glue in a high-Tc superconductor, Science 335, 1600 (2012).
- [5] C. Gadermaier, V. V. Kabanov, A. S. Alexandrov, L. Sto-jchevska, T. Mertelj, C. Manzoni, G. Cerullo, N. D. Zhigadlo, J. Karpinski, Y. Q. Cai, X. Yao, Y. Toda, M. Oda, S. Sugai, and D. Mihailovic, Strain-induced enhancement of the electron energy relaxation in strongly correlated superconductors, Phys. Rev. X 4, 011056 (2014).
- [6] F. Novelli, G. De Filippis, V. Cataudella, M. Esposito, I. Vergara, F. Cilento, E. Sindici, A. Amaricci, C. Giannetti, D. Prabhakaran, S. Wall, A. Perucchi, S. Dal Conte, G. Cerullo, M. Capone, A. Mishchenko, M. Grüninger, N. Nagaosa, F. Parmigiani, and D. Fausti, Witnessing the formation and relaxation of dressed quasiparticles in a strongly correlated electron system, Nature Communications 5, 5112 (2014).
- [7] J. D. Rameau, S. Freutel, L. Rettig, I. Avigo, M. Ligges, Y. Yoshida, H. Eisaki, J. Schneeloch, R. D. Zhong, Z. J. Xu, G. D. Gu, P. D. Johnson, and U. Bovensiepen, Photoinduced changes in the cuprate electronic structure revealed by femtosecond time- and angle-resolved photoemission, Phys. Rev. B 89, 115115 (2014).
- [8] J. D. Rameau, S. Freutel, M. A. Sentef, A. F. Kemper, J. K. Freericks, I. Avigo, M. Ligges, L. Rettig, Y. Yoshida, H. Eisaki, J. Schneeloch, R. D. Zhong, Z. J. Xu, G. D. Gu, P. D. Johnson, and U. Bovensiepen, Time-resolved boson emission in the excitation spectrum of Bi<sub>2</sub>Sr<sub>2</sub>CaCu<sub>2</sub>O<sub>8+δ</sub>, arXiv:1505.07055.
- [9] S. Dal Conte, L. Vidmar, D. Golež, M. Mierzejewski, G. Soavi, S. Peli, F. Banfi, G. Ferrini, R. Comin, B. M. Ludbrook, L. Chauviere, N. D. Zhigadlo, H. Eisaki, M. Greven, S. Lupi, A. Damascelli, D. Brida, M. Capone, J. Bonča, G. Cerullo, and C. Giannetti, Snapshots of the retarded interaction of charge carriers with ultrafast fluctuations in cuprates, Nature Physics 11, 421 (2015).
- [10] D. Golež, J. Bonča, L. Vidmar, and S. A. Trugman, Re-

- laxation dynamics of the Holstein polaron, Phys. Rev. Lett. 109, 236402 (2012).
- [11] G. De Filippis, V. Cataudella, E. A. Nowadnick, T. P. Devereaux, A. S. Mishchenko, and N. Nagaosa, Quantum dynamics of the Hubbard-Holstein model in equilibrium and nonequilibrium: Application to pump-probe phenomena, Phys. Rev. Lett. 109, 176402 (2012).
- [12] H. Matsueda, S. Sota, T. Tohyama, and S. Maekawa, Relaxation dynamics of photocarriers in one-dimensional Mott insulators coupled to phonons, J. Phys. Soc. Jpn. 81, 013701 (2012).
- [13] D. M. Kennes and V. Meden, Relaxation dynamics of an exactly solvable electron-phonon model, Phys. Rev. B 82, 085109 (2010).
- [14] A. F. Kemper, M. Sentef, B. Moritz, C. C. Kao, Z. X. Shen, J. K. Freericks, and T. P. Devereaux, Mapping of unoccupied states and relevant bosonic modes via the time-dependent momentum distribution, Phys. Rev. B 87, 235139 (2013).
- [15] M. Sentef, A. F. Kemper, B. Moritz, J. K. Freericks, Z.-X. Shen, and T. P. Devereaux, Examining electron-boson coupling using time-resolved spectroscopy, Phys. Rev. X 3, 041033 (2013).
- [16] P. Werner and M. Eckstein, Phonon-enhanced relaxation and excitation in the Holstein-Hubbard model, Phys. Rev. B 88, 165108 (2013).
- [17] V. V. Baranov and V. V. Kabanov, Theory of electronic relaxation in a metal excited by an ultrashort optical pump, Phys. Rev. B 89, 125102 (2014).
- [18] A. F. Kemper, M. A. Sentef, B. Moritz, J. K. Freericks, and T. P. Devereaux, Effect of dynamical spectral weight redistribution on effective interactions in time-resolved spectroscopy, Phys. Rev. B 90, 075126 (2014).
- [19] P. Werner and M. Eckstein, Field-induced polaron formation in the Holstein-Hubbard model, EPL (Europhysics Letters) 109, 37002 (2015).
- [20] Y. Murakami, P. Werner, N. Tsuji, and H. Aoki, Interaction quench in the Holstein model: Thermalization crossover from electron- to phonon-dominated relaxation, Phys. Rev. B 91, 045128 (2015).
- [21] F. Dorfner, L. Vidmar, C. Brockt, E. Jeckelmann, and F. Heidrich-Meisner, Real-time decay of a highly excited charge carrier in the one-dimensional Holstein model, Phys. Rev. B 91, 104302 (2015).
- [22] S. Sayyad and M. Eckstein, Coexistence of excited polarons and metastable delocalized states in photoinduced metals, Phys. Rev. B 91, 104301 (2015).
- [23] A. S. Mishchenko, N. Nagaosa, G. De Filippis, A. de Candia, and V. Cataudella, Mobility of Holstein polaron at finite temperature: An unbiased approach, Phys. Rev. Lett. 114, 146401 (2015).
- [24] V. Rizzi, T. N. Todorov, J. J. Kohanoff, and A. A. Correa, Electron-phonon thermalization in a scalable method for real-time quantum dynamics, Phys. Rev. B 93, 024306 (2016).
- [25] D. Golež, J. Bonča, M. Mierzejewski, and L. Vidmar,

- Mechanism of ultrafast relaxation of a photo-carrier in antiferromagnetic spin background, Phys. Rev. B 89, 165118 (2014).
- [26] E. Iyoda and S. Ishihara, Transient carrier dynamics in a Mott insulator with antiferromagnetic order, Phys. Rev. B 89, 125126 (2014).
- [27] M. Eckstein and P. Werner, Ultra-fast photo-carrier relaxation in mott insulators with short-range spin correlations, Scientific Reports 6, 21235 EP (2016).
- [28] D. Golež, M. Eckstein, and P. Werner, Dynamics of screening in photodoped mott insulators, Phys. Rev. B 92, 195123 (2015).
- [29] J. Bonča, S. A. Trugman, and I. Batistić, Holstein polaron, Phys. Rev. B 60, 1633 (1999).
- [30] L.-C. Ku, S. A. Trugman, and J. Bonča, Dimensionality effects on the Holstein polaron, Phys. Rev. B 65, 174306 (2002).
- [31] L. Vidmar, J. Bonča, M. Mierzejewski, P. Prelovšek, and S. A. Trugman, Nonequilibrium dynamics of the Holstein polaron driven by an external electric field, Phys. Rev. B 83, 134301 (2011).
- [32] D. Golež, J. Bonča, and L. Vidmar, Dissociation of a Hubbard-Holstein bipolaron driven away from equilibrium by a constant electric field, Phys. Rev. B 85, 144304 (2012).